Functional alteration of red blood cells by a megadalton protein of *Plasmodium falciparum*

Fiona K. Glenister,[1] Kate M. Fernandez,[1] Lev M. Kats,[1] Eric Hanssen,[2] Narla Mohandas,[3] Ross L. Coppel,[1] and Brian M. Cooke[1]

[1]Department of Microbiology, National Health and Medical Research Council Program in Malaria, Monash University, Victoria, Australia; [2]Centre of Excellence for Coherent X-ray Science and Department of Biochemistry, La Trobe University, Victoria, Australia; and [3]New York Blood Center, NY

Proteins exported from *Plasmodium falciparum* parasites into red blood cells (RBCs) interact with the membrane skeleton and contribute to the pathogenesis of malaria. Specifically, exported proteins increase RBC membrane rigidity, decrease deformability, and increase adhesiveness, culminating in intravascular sequestration of infected RBCs (iRBCs). Pf332 is the largest (>1 MDa) known malaria protein exported to the RBC membrane, but its function has not previously been determined. To determine the role of Pf332 in iRBCs, we have engineered and analyzed transgenic parasites with Pf332 either deleted or truncated. Compared with RBCs infected with wild-type parasites, mutants lacking Pf332 were more rigid, were significantly less adhesive to CD36, and showed decreased expression of the major cytoadherence ligand, PfEMP1, on the iRBC surface. These abnormalities were associated with dramatic morphologic changes in Maurer clefts (MCs), which are membrane structures that transport malaria proteins to the RBC membrane. In contrast, RBCs infected with parasites expressing truncated forms of Pf332, although still hyperrigid, showed a normal adhesion profile and morphologically normal MCs. Our results suggest that Pf332 both modulates the level of increased RBC rigidity induced by *P falciparum* and plays a significant role in adhesion by assisting transport of PfEMP1 to the iRBC surface. (Blood. 2009;113:919-928)

Introduction

A key feature in the pathogenesis of falciparum malaria is the parasite's ability to perturb the normal rheologic properties of the red blood cells (RBCs) that they invade. RBCs infected with mature stages of *Plasmodium falciparum* (infected RBCs [iRBCs]) are poorly deformable and adhere to the vascular endothelium. This grossly abnormal circulatory behavior results in the accumulation of iRBCs within the spleen and microvasculature, leading to life-threatening complications such as severe anemia and cerebral malaria.[1,2]

At the molecular level, these RBC modifications are mediated by a subset of parasite proteins that are exported across the parasitophorous vacuole membrane (PVM) into the RBC, where they then associate specifically with components of the RBC membrane skeleton. Many of these proteins carry a pentameric host-targeting signal sequence (termed vacuolar transport signal [VTS] or *Plasmodium* export element [PEXEL]) and are trafficked via parasite-induced membranous structures within the iRBC termed Maurer clefts (MCs).[3-5] *P falciparum* erythrocyte membrane protein 1 (PfEMP1) is the major adhesion ligand that is exposed on the iRBC surface that can bind to a number of receptors expressed on vascular endothelial cells, including CD36.[1] Other proteins, such as the knob-associated histidine-rich protein (KAHRP), mature parasite-infected erythrocyte surface antigen (MESA), and PfEMP3, are localized on the cytosolic side of the iRBC membrane. By forming specific protein-protein interactions with components of the RBC membrane skeleton, they anchor PfEMP1 into the RBC membrane and alter the mechanical properties of iRBCs.[6-8]

P falciparum antigen 332 (Pf332) is encoded by a gene of approximately 20 kb and is the second largest protein in the *P falciparum* proteome with an observed molecular mass of > 1 MDa.[9] It is composed of a Duffy binding-like (DBL) domain at the N terminus of the protein and a large number of highly degenerate glutamic acid–rich repeats in the C-terminal domain.[10] During the early stages of parasite development, Pf332 is localized at the PVM and in MCs and, in later stages, also associates with the iRBC membrane skeleton.[9,11] To date, few studies have focused on Pf332, and its function within iRBCs remains unknown. It has been suggested that Pf332 is partially exposed on the surface of iRBCs and anti-Pf332 antibodies have been shown to inhibit both parasite growth and cytoadherence in vitro.[9,10,12,13] However, localization studies of RBCs containing very mature parasites are known to be problematic because increased permeability of the RBC membrane can allow antibodies access to parasite proteins on the cytoplasmic face of the membrane,[11] which may in fact explain how anti-Pf332 antibodies enter mature iRBCs and interfere with normal parasite development and inhibition of parasite release from these cells in vitro.[13]

In an attempt to determine the function of Pf332 in iRBCs, we have created a number of independent transgenic parasite lines in which the *Pf332* gene was either deleted or truncated. Interestingly, Pf332 appears to have a dual function in iRBCs, regulating both the extent of parasite-induced membrane rigidification and the cells' adhesive properties. Our data identify Pf332 as an important player
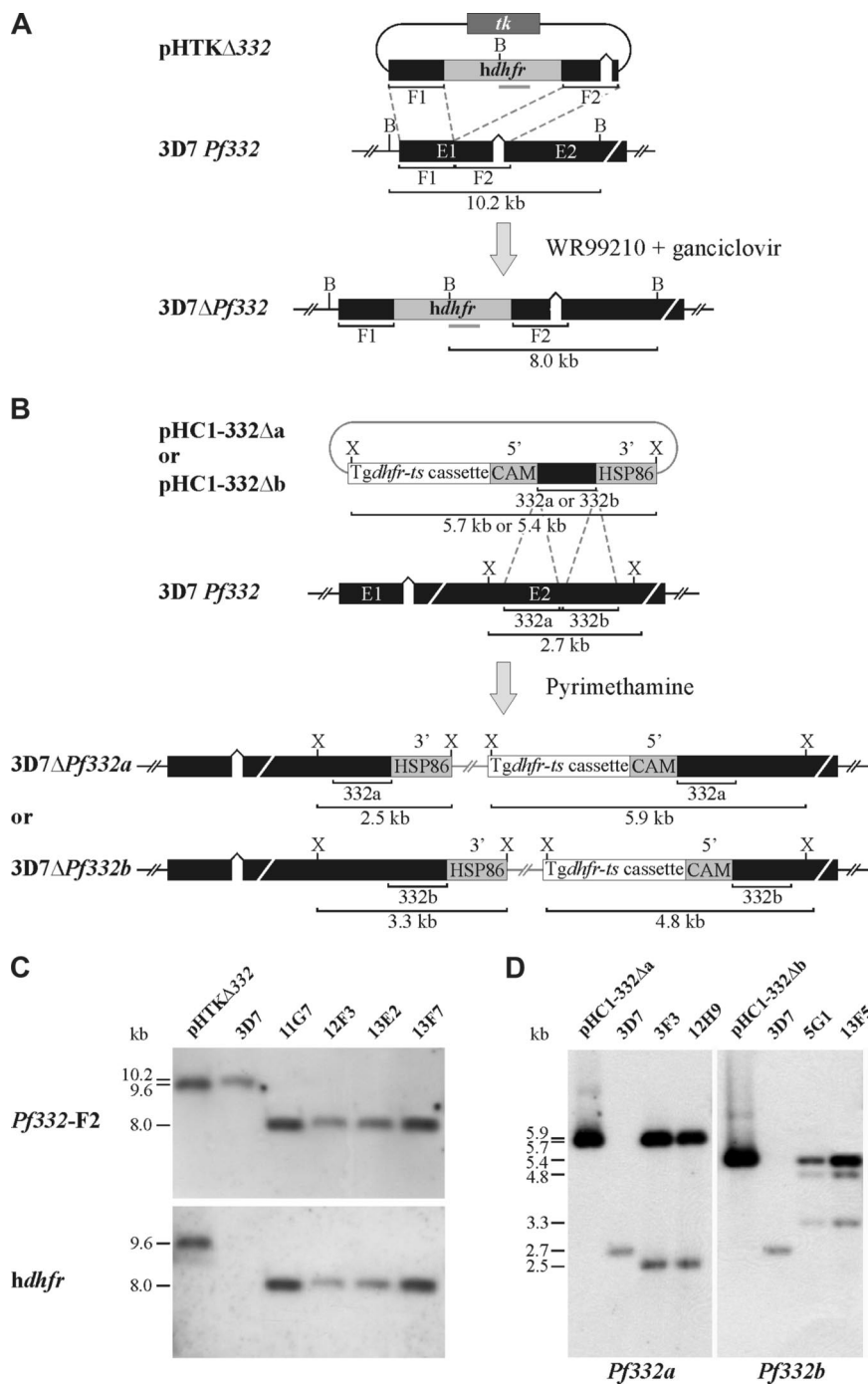
Figure 1. Pf332 transfection constructs and integration events. (A) Schematic representation of the pHTKΔ332 transfection plasmid and disruption of the *Pf332* gene (3D7 *Pf332*) in *P falciparum* 3D7 parasites. The proposed model of the *Pf332* gene locus disrupted by incorporation of the h*dhfr* resistance cassette in drug-resistant transgenic KO parasites is also shown (3D7ΔPf332). The position of relevant restriction enzyme sites for *Bam*HI (B), the expected sizes of restriction fragments, and the position of the h*dhfr* probe (gray bar) are shown. (B) Schematic representation of the pHC1-332Δa and pHC1-332Δb transfection plasmids and the site of targeted disruption of the *Pf332* gene (3D7 *Pf332*) in 3D7 parasites. The proposed models of integration of both plasmids into the *Pf332* gene (3D7ΔPf332a/3D7ΔPf332b) are also shown. The position of relevant restriction enzyme sites for *Xba*I (X) and the expected sizes of restriction fragments are shown. (C) Southern blot analysis of *Bam*HI-digested pHTKΔ*332* and genomic DNA from 3D7 and the 4 3D7ΔPf332 KO clones: 11G7, 12F3, 13E2, and 13F7. Hybridization of the Pf332-F2 and h*dhfr* probes to digested DNA from all 3D7ΔPf332 parasite clones revealed restriction fragment sizes consistent with the disruption of *Pf332* by double crossover homologous recombination and incorporation of the h*dhfr* drug resistance cassette. (D) Southern blot analysis of *Xba*I-digested pHC1-332Δa, pHC1-332Δb, and genomic DNA from 3D7 and the 3D7ΔPf332a (3F3 and 12H9) and 3D7ΔPf332b (5G1 and 13F5) clones. Hybridization of the Pf332a and Pf332b probes to digested DNA from the 3D7ΔPf332a and 3D7ΔPf332b clones, respectively, revealed restriction fragment sizes consistent with the disruption of *Pf332* by single crossover homologous recombination and incorporation of the entire transfection plasmids.

in the modification of RBCs and ultimately the pathogenesis of falciparum malaria.

Methods

Malaria parasites

P falciparum parasites (3D7 clone) were maintained in continuous in vitro culture in human RBCs suspended in HEPES (*N*-2-hydroxyethylpiperazine-*N*′-2-ethanesulfonic acid)–buffered RPMI 1640 medium supplemented with 0.5% Albumax II using standard procedures.[14] Cultures were kept synchronous, and the knob-positive phenotype was maintained by weekly flotation in gelatin as previously described.[15] Clonal parasite lines were derived from transfected 3D7 parasite lines by limiting dilution (Figure S1,

available on the *Blood* website; see the Supplemental Materials link at the top of the online article).

Plasmid constructs

To disrupt the *Pf332* gene in 3D7 parasites, 2 sequences (~1 kb) from the 5′ end of exon 1 of *Pf332* were cloned into the *P falciparum* transfection plasmid pHHT-TK[16] (a gift from Profs A. Cowman and B. Crabb, The Walter and Eliza Hall Institute of Medical Research, Melbourne, Australia) to derive pHTKΔ*332* (Figure 1A). Specifically, the first segment of *Pf332* was amplified from genomic DNA from 3D7 parasites with the forward and reverse primers 5′TCC**CCGCGG**gaatctgtctaatataaataactaaga3′ (*Sac*II site in bold) and 5′GG**ACTAGT**ctatgaaatttatctactaat3′ (*Spe*I site in bold), respectively, and subcloned into the *Sac*II and *Spe*I sites of pHHT-TK upstream of the human dihydrofolate reductase (h*dhfr*) drug-resistance

cassette. The second segment, located 40 bp downstream of the first, was amplified with the use of forward and reverse primers 5′CC**ATCGAT**gatgaattaaatcgtgataat3′ (*Cla*I site in bold) and 5′CATG**CCATGG**cattattttttctatttcgttct3′ (*Nco*I site in bold) respectively, and introduced into the *Cla*I and *Nco*I sites downstream of h*dhfr*.

To disrupt the *Pf332* gene to allow for the expression of a truncated Pf332 protein product, 2 slightly overlapping regions of approximately 1 kb were cloned separately into the *Xho*I site of the *P falciparum* transfection plasmid pHC1[17] to derive pHC1-332Δa and pHC1-332Δb (Figure 1B). The target sequences for pHC1-332Δa and pHC1-332Δb were amplified from 3D7 genomic DNA with the use of forward and reverse primers 5′CCG**CTCGAG**acgaattccggaacaagaagg3′ and 5′CCG**CTCGAG**ctcagcatctgattctttgtttat3′ and 5′CCG**CTCGAG**gttcaagatggattaattaca3′ and 5′CCG**CTCGAG**agtaagtgattttttcgtcaat3′ (restriction sites in bold) for a and b, respectively, and introduced into the *Xho*I site flanked by the calmodulin (CAM 5′) promoter and the heat-shock protein 86 (HSP86 3′) terminator sequences. Both inserts were in the forward orientation with respect to the drug-resistance cassette.

Parasite transfection

Ring-stage parasites were transfected with 150 µg plasmid DNA by electroporation as described previously.[18] For targeted gene knockout (KO), parasites transformed with pHTKΔ332 were cultured in the presence of 2.5 nmol/L WR99210 for approximately 30 days until viable parasites were observed in blood smears stained with Giemsa. Ganciclovir (4 µmol/L; Roche, Dee Why, Australia) was then added to select for parasites having only double crossover homologous recombination.[16] For truncation of *Pf332*, positive selection for parasites transformed with pHC1-332Δa/b was performed using 0.1 µmol/L pyrimethamine (Sigma-Aldrich, Sydney, Australia) initially as previously described.[19] The concentration of pyrimethamine was then increased to 1 µmol/L after drug cycling.

DNA extraction and Southern blotting

Genomic DNA was extracted from parasite culture with the Nucleon BACC2 Kit (Amersham Pharmacia Biotech, Buckinghamshire, United Kingdom), digested with *Xba*I, separated on 1% agarose gels, and transferred to nylon membrane. Southern blot hybridization and analysis was performed with the use of standard procedures.

Western blotting

Cultured iRBCs were harvested on Percoll and membrane proteins were extracted with the use of Triton X-100 and SDS solubilization as described previously and diluted in reducing Laemmli sample buffer. Total parasite extracts were then separated on 5% sodium dodecyl sulfate–polyacrylamide gel electrophoresis (SDS-PAGE) gels and transferred to polyvinylidene difluoride (PVDF) membranes. Membranes were probed with rabbit polyclonal anti-HSP70 (1: 10 000) or mouse polyclonal anti-Pf332 N-terminal or C-terminal antibodies (1:150). Detection by chemiluminescence (Lumi-light Western blotting substrate; Roche Diagnostics) was performed after a secondary probe with either sheep anti–rabbit or sheep anti–mouse immunoglobulin (Ig)–HRP conjugate (1:2000; Chemicon, Melbourne, Australia).

Indirect immunofluorescence assays

Indirect immunofluorescence was conducted either on thin culture smears that had been air-dried and fixed with cold acetone/methanol (9:1) or on cultured iRBCs that had been fixed with paraformaldehyde and then permeabilized with equinatoxin II[20] in suspension as recently described.[21] Smears or RBC suspensions were then incubated for 1 hour with either mouse polyclonal anti-Pf332E1 (N-terminal; 1:100), mouse polyclonal anti-Pf332F19 (C-terminal; 1:100), rabbit polyclonal anti-SBP1 (1:500), rabbit polyclonal anti-KAHRP (1:500), rabbit polyclonal anti-VARC (1: 100), or mouse polyclonal anti-SBP1 (1:500). Primary antibodies were detected by incubation for 1 hour with anti–mouse or anti–rabbit IgG conjugated to Alexa Fluor 488 or Alexa Fluor 568 (1:1000; Invitrogen, Carlsbad, CA). Slides were mounted in VECTASHIELD (Vector Laboratories, Burlingame, CA) containing 2 µg/mL 4′,6-diamidino-2-phenylindole

(DAPI) and visualized on a fluorescence microscope (BX51; Olympus, Melbourne, Australia).

Electron microscopy

To examine the ultrastructure of MCs by electron microscopy, RBCs from cultures containing predominantly mature-stage parasites were fixed, stained, and sectioned with the use of routine preparative techniques as previously described.[22] In brief, cultured RBCs were fixed with glutaraldehyde, postfixed with osmium tetroxide, and then stained en-bloc with uranyl acetate before they were embedded in LR White resin (London Resin, Berkshire, United Kingdom). After sectioning, samples were stained with uranyl acetate and lead citrate and observed with a JEOL 2010HC electron microscope at 80 kV. Digital images were captured with a Veleta (2k × 2k) side-mounted transmission electron microscopy (TEM) camera (Olympus Soft Imaging System, Munster, Germany).

Measurement of membrane shear elastic modulus by micropipette aspiration

Single-cell micropipette aspiration was used to determine the shear elastic modulus of RBC membranes as previously described.[7] In brief, the membrane of individual RBCs was aspirated progressively into prefabricated glass micropipettes (internal diameter 1.2-1.4 µm) over a range of increasing negative suction pressures. Membrane shear elastic modulus was determined by measuring the length of a membrane tongue (L) aspirated from the RBC into the pipette for a range of aspiration pressures (P) and calculated from the linear regression of dL/dP. The range of aspiration pressures was 1.0 to 4.0 mm H_2O for uninfected RBCs or 1.0 to 14.0 mmH_2O for iRBCs. All measurements were performed at room temperature (approximately 20°C-25°C).

Measurement of RBC adhesive properties

Adhesion of iRBCs to CD36, either purified or expressed on the surface of platelets, was quantified under both static and flow conditions. Parasite cultures were tested when the majority of parasites were pigmented trophozoites as assessed by Giemsa-stained smears. In each adhesion experiment, cultured 3D7-iRBCs and one or more of the transgenic parasite lines were resuspended in adhesion buffer (HEPES-buffered RPMI 1640 supplemented with 1% bovine serum albumin [BSA] and pH adjusted to 7.0) to a concentration of 3×10^8 RBCs/mL for static adhesion assays or 1.5×10^8 RBCs/mL for flow-based assays, and the parasitemia of the suspensions equalized (average 3.5% trophozoites; range, 3%-5.2% for all experiments performed).

For static adhesion assays, platelet monolayers were prepared in small sections circumscribed with a hydrophobic pen on acid-washed glass coverslips. Adhesion of 3D7 and one transgenic clone to the platelet monolayers was compared on a single glass coverslip as previously described.[23] Measurement of iRBC adhesion under physiologically relevant flow was performed with a competitive, fluorescent microcapillary method as previously described[24] so that the adhesion of RBCs infected with parental 3D7 parasites could be compared directly with RBCs infected with transgenic Pf332 clones in a single assay. Cell suspensions were flowed under conditions that mimic those in postcapillary venules through flat, rectangular, glass microcapillary tubes (Microslides; VitroCom, Mountain Lakes, NJ), coated with purified CD36 or platelet monolayers with the use of a flow-control system as previously described.[25,26] Adherent iRBCs were visualized and quantified by direct microscopic observation (IMT-2; Olympus) with a 40× water-immersion objective (Olympus) and the relative proportions of adherent iRBCs infected with either parental 3D7 parasites or a transgenic clonal line determined.

Analysis of PfEMP1 on the surface of iRBCs by trypsin cleavage assay

Trypsin cleavage assays were performed to detect PfEMP1 expressed on the surface of iRBCs as previously described.[27] In brief, mature iRBCs were enriched on Percoll then incubated with 100 µg/mL TPCK-treated trypsin (Sigma-Aldrich) in the presence or absence of 1 mg/mL soybean trypsin

inhibitor (STI; Sigma-Aldrich) for 15 minutes at 37°C. Trypsin activity was then ablated by the addition of STI to a final concentration of 1 mg/mL followed by a further incubation at room temperature for 15 minutes. RBC membrane skeleton-associated proteins (including PfEMP1) were extracted with the use of Triton X-100 and SDS solubilization as described previously and diluted in reducing Laemmli sample buffer.[27] Samples were separated on 6% SDS-PAGE gels and transferred for 4 hours at 4°C onto PVDF. The cytoplasmic tail of PfEMP1 (VARC) was detected with mouse monoclonal antibody 1B/98-6H1-1 (1:100; The Walter and Eliza Hall Institute Monoclonal Antibody Facility, Bundoora, Australia).

Results

Disruption of the *Pf332* locus and generation of mutant parasite clones

Pf332 (PlasmoDB gene identification number PF11_0507) is approximately 20 kb in length and is located in the subtelomeric region of *P falciparum* chromosome 11. To investigate the role of Pf332 in the structural and functional modification of iRBCs, we generated stable transgenic *P falciparum* clones (from the 3D7 parasite clone) in which *Pf332* was disrupted (Figure S1). Integration of the h*dhfr* drug cassette into *Pf332* by double crossover homologous recombination disrupted the coding region at residue 341, resulting in loss of the majority of the *Pf332* coding sequence (Figure 1A). Four clonal lines (11G7, 12F3, 13E2, and 13F7) from 2 independent transfection events were obtained by limiting dilution (Figure S1). Analysis by Southern blotting of genomic DNA digested with *Bam*HI and probed with either *Pf332*-F2 or h*dhfr* confirmed that *Pf332* had been disrupted in all 4 parasite clones (Figure 1A,C). Similar results were obtained on Southern blots using genomic DNA digested with *Xba*I (data not shown). Because our KO strategy had interrupted the coding region of *Pf332* at residue 341, we performed reverse-transcription polymerase chain reaction (RT-PCR) to rule out the possibility that approximately the first 35 kDa of *Pf332* was expressed in the KO clones. Complementary DNA (cDNA) from parental 3D7 parasites and all 4 KO clones, generated using a *Pf332* specific primer or oligo-dT, respectively, was subjected to PCR with primers specific for the extreme 5′ end of the *Pf332* gene. No PCR product was detected for any of the KO mutants, whereas a product of the expected size was observed for 3D7 (Figure S2). This finding confirmed that *Pf332* transcription was completely ablated in the KO parasite lines. No episomal plasmid could be detected in any of the clones by PCR analysis (data not shown).

We also generated transgenic parasite lines in which *Pf332* was truncated. This strategy was designed so that integration of either pHC1-332Δa or pHC1-332Δb into *Pf332* by single crossover homologous recombination would disrupt the coding region at residues 2965 and 3246, respectively (Figure 1B). After drug cycling to eliminate episomal plasmid and cloning by limiting dilution, 2 clones for each construct (3F3 and 12H9 for pHC1-332Δa; and 5G1 and 13F5 for pHC1-332Δb) were selected (Figure S1B). Southern blotting (Figure 1B,D) and PCR analysis (data not shown) confirmed that integration had occurred as expected.

Characterization of Pf332 deletion and truncation mutant parasites

The transgenic parasite clones were analyzed for Pf332 expression by Western blotting using polyclonal antibodies raised against the extreme NH$_2$-terminal region of Pf332 (Figure 2A). In RBCs infected with parental 3D7 parasites, Pf332 was detected as a high-molecular-weight band migrating well above the 250-kDa marker. A number of smaller bands were also observed, which are likely to be processed or
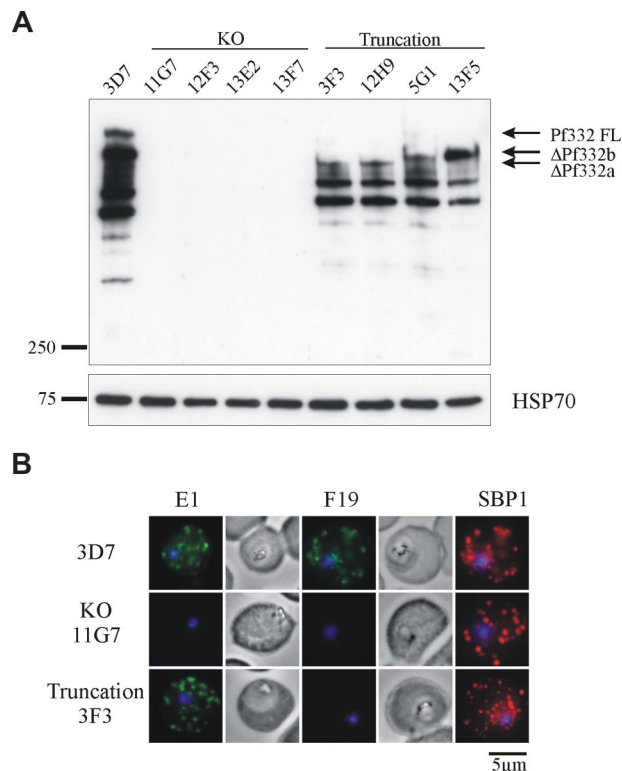

Figure 2. Expression of Pf332 is abolished in 3D7ΔPf332 KO clones or expressed as a smaller, truncated protein in 3D7ΔPf332a and 3D7ΔPf332b clones. (A) Western blot analysis of Pf332 expression in 3D7 parasites, 3D7ΔPf332 KO clones (11G7, 12F3, 13E2, and 13F7), and the 3D7ΔPf332a (3F3 and 12H9) and 3D7ΔPf332b (5G1 and 13F5) clones. Membranes were probed with antibodies raised against the NH$_2$-terminal region of Pf332. Bands corresponding to full-length Pf332 (Pf332FL), or the size-truncated proteins ΔPf332b and ΔPf332a are indicated. An identical blot was probed for HSP70 as a parasite loading control. Densitometric quantitation with NIH ImageJ open source software (National Institutes of Health, Bethesda, MD) of total Pf332 reactivity for 3D7 and each of the truncation mutants (corrected for equal loading of iRBCs) revealed that all mutants express similar levels of protein, which was approximately half the amount of full-length Pf332 expressed by 3D7 parasites (total Pf332 expressed as percentage of 3D7 = 41%, 39%, 53%, and 44% for clones 3F3, 12H9, 5G1, and 13F5, respectively). (B) Immunofluorescence analysis of iRBCs infected with 3D7, 3D7ΔPf332 (11G7), or 3D7ΔPf332a (3F3). iRBCs were incubated with antibodies raised against the N-terminal (E1) or C-terminal (F19) regions of Pf332, or with the MC marker SBP1. Note that no fluorescence of the MCs or iRBC membrane could be detected in the 3D7ΔPf332 KO clones. Parasite nuclei were counterstained with DAPI.

proteolytic breakdown products of the full-length protein because they were not detected in the KO lines. As expected, all 4 KO clones showed no reactivity of any bands with the Pf332 antibody, confirming that Pf332 expression had been completely ablated. In each of the truncated clones, a partial, smaller Pf332 protein was observed that also migrated above the 250-kDa marker but below full-length Pf332.

As expected, clones 3F3 and 12H9 expressed a smaller protein product than clones 5G1 and 13F5. Densitometric quantitation of total Pf332 reactivity from 3D7 and each of the truncation mutants revealed that all mutants expressed similar, yet reduced levels of the truncated Pf332 protein. When adjusted for differences in loading between parasite samples, with reactivity of *P falciparum* heat shock protein 70 (HSP70) as a loading control, the mean level of truncated Pf332 expressed in all mutants was 44% of the level of full-length protein expressed by 3D7 parasites (range, 39-53%; Figure 2).

3D7 and transgenic parasite lines were further analyzed by immunofluorescence. Results for 1 representative KO line (11G7) and 1 truncated Pf332 line (3F3) are shown (Figure 2B). We used antibodies raised against either the NH$_2$ terminus (E1) or the COOH terminus (F19) of Pf332. Both antibodies revealed a punctate pattern of fluorescence in the

Figure 3. Abnormal morphology of MCs is observed in RBCs infected with mature-stage parasites. (A) Immunofluorescence analysis of 3D7 or 3D7ΔPf332 (11G7 or 13E2) schizont-infected RBCs containing 8 or more DAPI-stained nuclei. MCs were visualized with antibodies raised against SBP1. Greater than 60% of transgenic Pf332KO iRBCs showed fewer and abnormally large MCs compared with 3D7 iRBCs. A total of 2 typical iRBCs are shown for each parasite line. (B) Electron micrographs of thin sections through RBCs infected with late-stage parasites (P), either the parental line (3D7) or the Pf332 KO clone (11G7), showing the ultrastructure and arrangement of Maurer clefts (MC) underlying the RBC membrane (RBCM). Note that MCs are stacked and aggregated in the absence of Pf332.
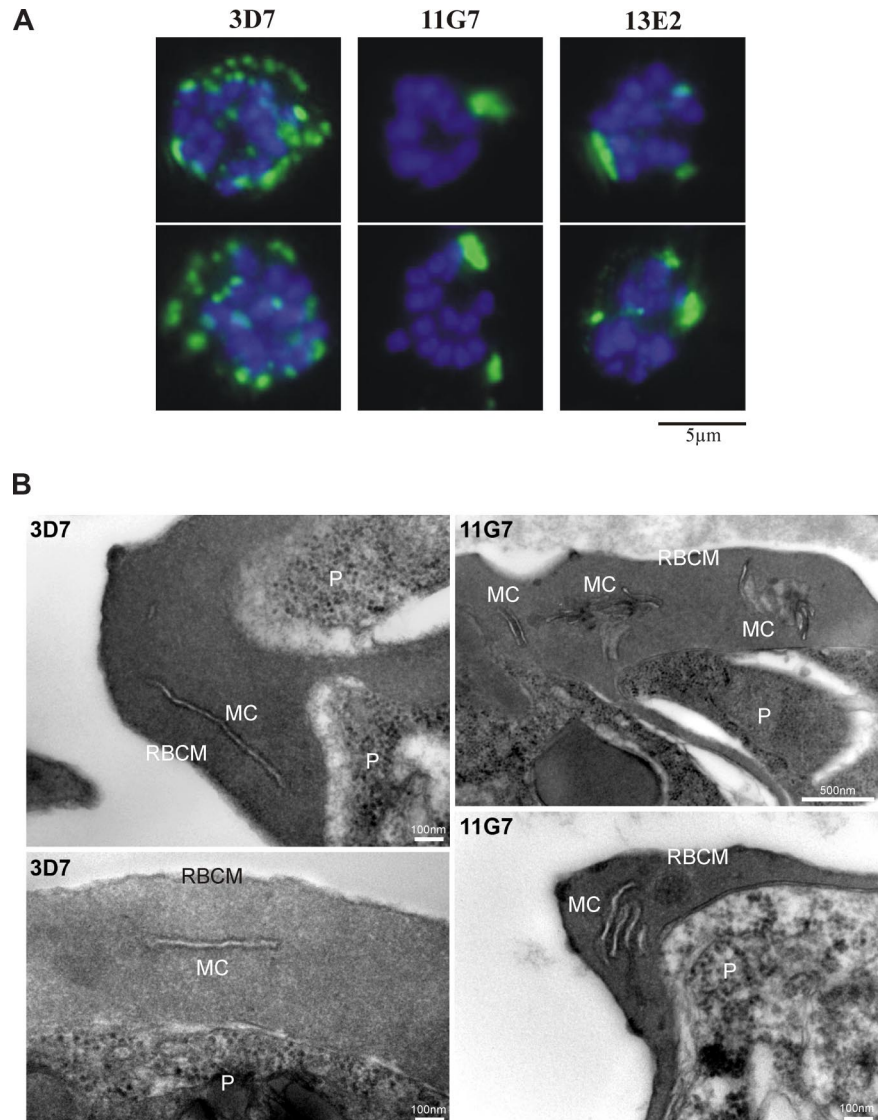
cytoplasm of 3D7 iRBCs typical of MCs that colocalized with the MC marker SBP1. No reactivity with either E1 or F19 antibodies was observed for Pf332 KO iRBCs, confirming that reactivity was specific for Pf332. RBCs infected with truncated parasite lines reacted only with E1 antibodies and produced the same pattern observed for 3D7, indicating that the truncated Pf332 product was correctly trafficked to MCs, where it colocalized with SBP1.

Because Pf332 is an extremely large protein, its absence may influence the binding or localization of other parasite proteins exported into the RBC. We examined the localization of the knob-associated histidine-rich protein (KAHRP), which is the major structural component of membrane knobs on iRBCs, and found that there was no difference in the pattern of KAHRP fluorescence between wild-type parasites and all transgenic clones (results not shown). Similarly, analysis of the number and morphologic appearance of membrane knobs with atomic force microscopy showed no apparent differences between RBCs infected with either wild-type or transgenic parasites for all of the parasite clones generated, either truncated or KO (C.-T. Lim and Ang Li, National University of Singapore, e-mail communication, February 13, 2008).

Interestingly, however, we observed that the morphology of MCs (as defined by SBP1 fluorescence) was altered in RBCs infected with Pf332 KO clones compared with MCs in 3D7- or

truncation mutant–infected RBCs. This defect was particularly apparent in mature parasite (schizont)–infected RBCs, where MCs were less numerous and much larger in the Pf332 KO (Figure 3A). Quantitation of MCs in RBCs infected with mature schizont-stage parasites with 8 or more DAPI-stained nuclei showed that for the Pf332 KO parasite lines, > 60% of iRBCs displayed this abnormal cleft phenotype. A more detailed examination of RBCs infected with Pf332 KO parasites by electron microscopy revealed the ultrastructural basis for this unusual MC phenotype. In the absence of Pf332, MCs underlying the RBC membrane were highly aggregated and formed multilamellar stacks rather than individual lamellae that are displayed by wild-type 3D7 parasites (Figure 3B).

Pf332 modulates parasite-induced rigidification of the iRBC membrane

To determine the contribution of Pf332 to the altered mechanical properties of the RBC membrane skeleton, we measured and compared the shear elastic modulus of normal uninfected RBCs and RBCs infected with either parental 3D7 parasites or transgenic parasite lines (Figure 4). As expected, infection of RBCs with 3D7 parasites caused a significant increase in the rigidity of the RBC
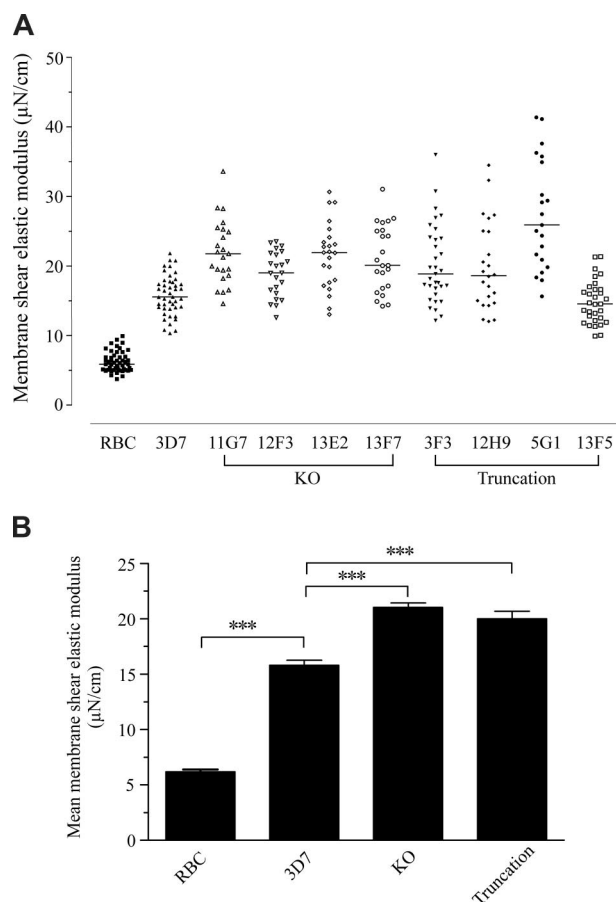
A

Figure 4. Disruption or truncation of *Pf332* affects the membrane shear elastic modulus of RBCs infected by mature stages of *P falciparum*. (A) Membrane shear elastic modulus of uninfected RBCs and iRBCs from 3D7, 3D7Δ*Pf332* (11G7, 12F3, 13E2, and 13F7), 3D7Δ*Pf332*a (3F3 and 12H9), and 3D7Δ*Pf332*b (5G1 and 13F5) quantified by single-cell micropipette aspiration. Each point represents the membrane shear elastic modulus for an individual RBC. Horizontal bars represent the median of all data in each group. (B) Data for individual RBCs shown in panel A pooled by group to more clearly indicate the overall level (mean + SEM) of membrane rigidification induced by either 3D7, Pf332 knockout (KO), or Pf332 truncation mutant (Truncation) parasites. The shear elastic modulus for normal, uninfected RBCs is shown for comparison (RBC). *** indicates significant differences between groups ($P < .001$ by one-way analysis of variance).

Figure 5. Disruption of *Pf332* reduces CD36-mediated adhesion of iRBCs to human platelets under flow and static conditions. Level of adhesion of iRBCs to purified or cell-expressed CD36 from KO 3D7Δ*Pf332* (11G7, 12F3, 13E2, and 13F7), truncation 3D7Δ*Pf332*a (3F3 and 12H9), and truncation 3D7Δ*Pf332*b (5G1 and 13F5) cultures measured under flow or static conditions. Adhesion represents the number of iRBCs that adhered for the transgenic parasite clones as a percentage of wild-type 3D7 iRBCs. In all assays, adhesion of noninfected RBCs was rare ($< 0.05\%$ of total adherent RBCs). Data represent the mean plus or minus SEM (error bars) for at least 3 independent experiments for each parasite clone.

membrane ($P < .001$ by one-way analysis of variance [ANOVA]) and, on average, the elastic modulus of 3D7 iRBCs was 2.6 times greater than that of uninfected RBCs. Notably, the elastic modulus of RBCs infected with either the Pf332 truncation or KO mutants was even greater than that of 3D7 iRBCs, with an average increase of 3.2 and 3.4 times, respectively, compared with the uninfected RBC control ($P < .001$ by one-way ANOVA; Figure 4B). Furthermore, on average, there was no statistically significant difference between the increases in membrane rigidity caused by either the KO or truncation parasites (Figure 4B). The range of the data for each of the transgenic lines was also greater than for the 3D7 parental line. These data imply that Pf332 plays a role in modulating the overall rigidification of the iRBC membrane that is induced by *P falciparum* infection.

Pf332 KO parasites demonstrate reduced adhesion under static and flow conditions

Cytoadherence of iRBCs to the vascular endothelium is dependent upon correct presentation and anchoring of PfEMP1 at the RBC surface. To determine the role of Pf332 in modulating adhesive
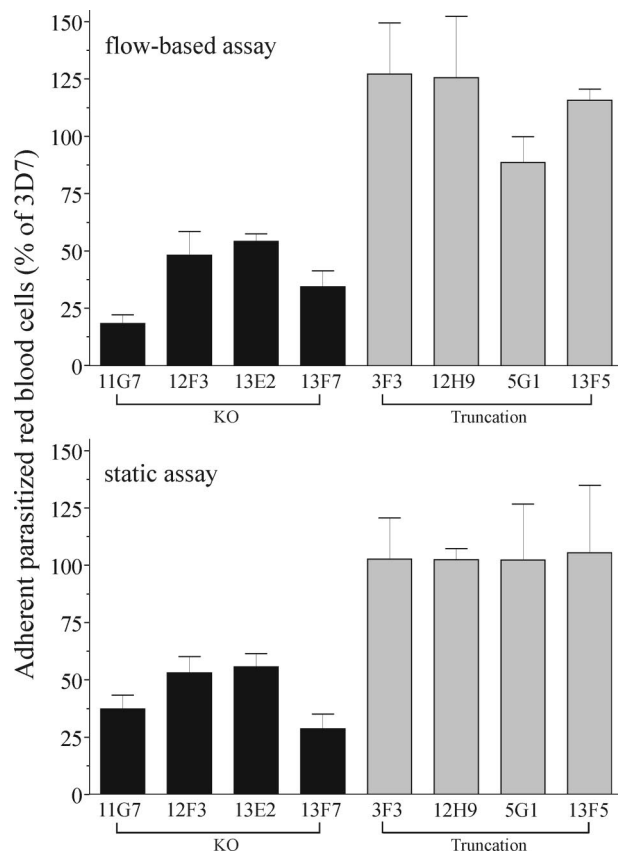
properties of iRBCs, we quantified the ability of RBCs infected with either wild-type or transgenic parasites to adhere to immobilized, recombinant CD36 or confluent monolayers of human platelets (expressing CD36 on their surface; Figure 5). Adhesion of RBCs infected with any of the Pf332 KO clones (11G7, 12F3, 13E2, 13F7) was significantly reduced compared with 3D7 parasites under both flow and static conditions (median reduction in adhesion for all KO clones = 61.5% and 55.2% in flow and static assays, respectively; minimum of 3 comparisons for each of the 4 clones; $P < .05$ by Kruskal-Wallis test). In contrast, adhesion of RBCs infected with any of the 4 truncated clones was not significantly different to 3D7. Taken together, these data indicate that the N-terminal region of the Pf332 protein upstream of residue 2965 is involved in alteration of the adhesive properties of iRBCs, presumably by affecting trafficking of PfEMP1 to the iRBC surface.

Trafficking of PfEMP1 to the iRBC surface is reduced in Pf332 KO parasites

To investigate whether reduced adhesion of Pf332 KO iRBCs was caused by a reduction in the amount of PfEMP1 exposed on the iRBC surface, trypsin cleavage assays were performed (Figure 6).[27] Because RBCs infected with Pf332-truncated parasite lines showed normal levels of adhesion, they were not analyzed by this method.
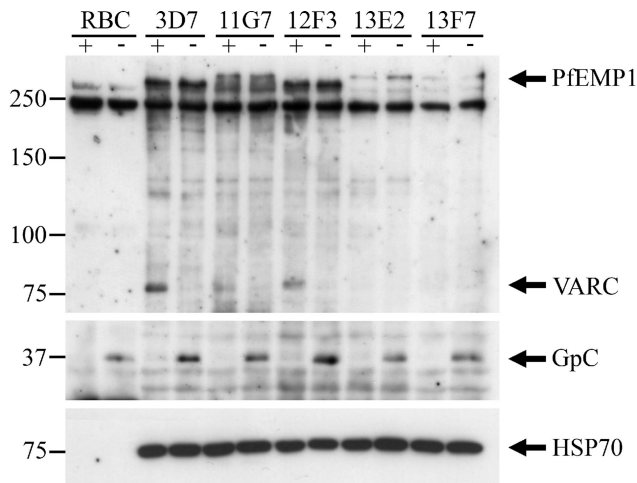
Figure 6. Surface-exposed PfEMP1 is reduced in *Pf332* KO parasite lines. Western blot analysis of Triton X-100-insoluble/SDS-soluble membrane fractions from uninfected RBCs or iRBCs (3D7, 3D7Δ*Pf332* [11G7, 12F3, 13E2, and 13F7]), either with (+) or without (−) treatment with trypsin. The 2 bands below full-length PfEMP1 at approximately 250 kDa represent cross-reactivity with the RBC cytoskeletal proteins α and β spectrin. The approximately 80-kDa band detected after treatment with trypsin (VARC) represents the cytoplasmic domain of surface-exposed PfEMP1 in these iRBCs. An identical blot was probed for HSP70 as a parasite-loading control and with anti–glycophorin C (GpC) as a control for digestion of RBC surface proteins.

Trypsin treatment of intact iRBCs results in proteolysis of the exodomain of PfEMP1, leaving intact the approximately 80-kDa cytoplasmic tail (VARC), which can be detected with a VARC-specific antibody. Western blot analysis of trypsin-treated iRBCs was conducted 3 times. In each case, surface-exposed PfEMP1 was shown to be reduced, as evidenced by the absence or reduction of the 80-kDa trypsin-resistant cytoplasmic tail of PfEMP1 in the KO lines compared with the parental control (Figure 6). Immunofluorescence analysis of Pf332 KO iRBCs using the anti-VARC antibody revealed that PfEMP1 was still localized in MCs and its intracellular distribution did not appear different from 3D7-infected RBCs (Figure 7). Taken together, these results suggest that Pf332 plays a role in the translocation of PfEMP1 from MCs to the RBC surface.

Discussion

As *P falciparum* malaria parasites develop and mature, they progressively modify the unique rheologic properties of the RBCs in which they reside. iRBCs are poorly deformable, highly rigid, and show an abnormal propensity to adhere to vascular endothelial cells. As a consequence of their altered rheologic properties, iRBCs cease to circulate normally and become sequestered in the microvasculature of most, if not all, organs of the body, resulting in
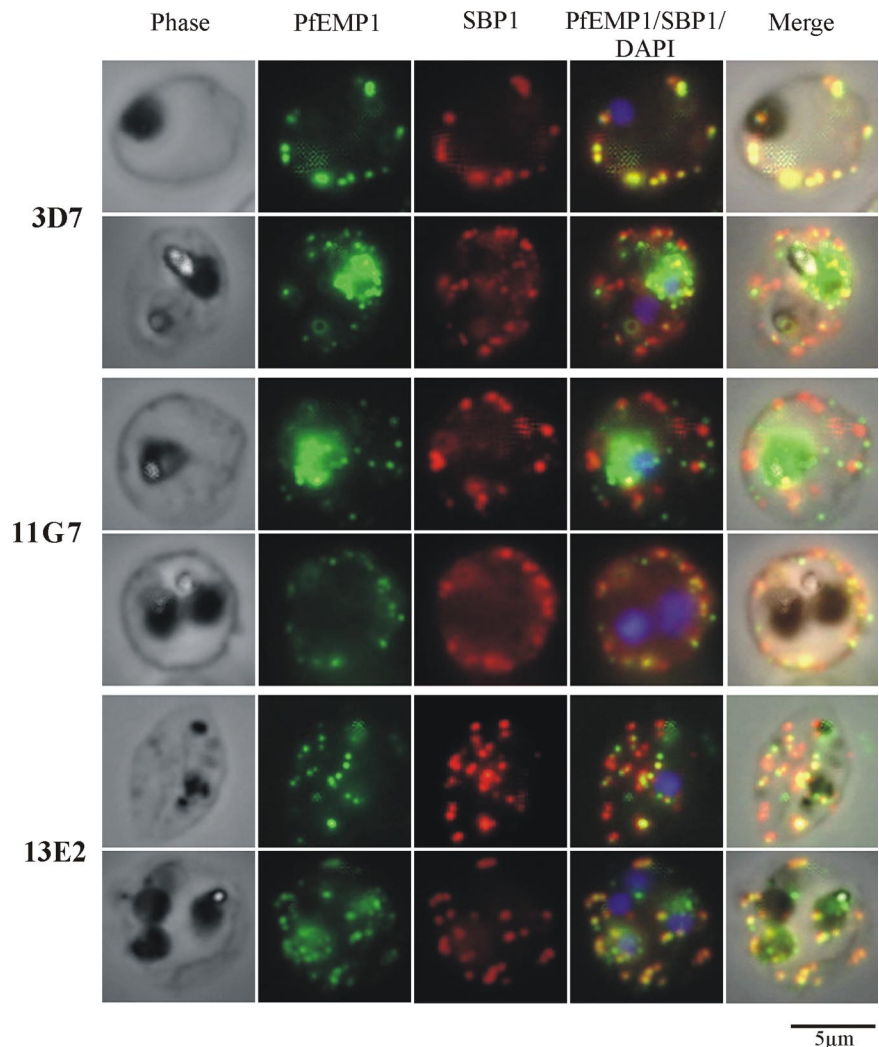

Figure 7. PfEMP1 is correctly trafficked to MCs in *Pf332* KO lines. Immunofluorescence analysis of 3D7 or 3D7Δ*Pf332* (11G7 or 13E2) iRBCs with anti-VARC antibody shows punctate PfEMP1 fluorescence consistent with its localization in MC. Double labeling with anti-VARC (green) and anti-SBP1 (red) antibodies shows coresidence of PfEMP1 in some (but not all) of SBP1-positive MCs. A total of 2 representative RBCs are shown for each transgenic parasite line and show no detectable difference between the intracellular localization of PfEMP1 in 3D7 parasites or either of the Pf332 KO clones.

5μm

often-fatal clinical complications. These changes to the mechanical and adhesive properties of iRBCs are the consequence of direct and indirect interactions of exported parasite proteins with the RBC membrane skeleton. Analysis of the genome sequence of *P falciparum* suggests that the repertoire of proteins exported into the RBC is large (~400),[28] yet, to date, only a relatively small number of these have been characterized and their function in iRBCs determined.

Because the membrane skeleton that underlies the lipid membrane of RBCs plays a fundamental role in determining their shape and deformability, it is not surprising that interaction of exported parasite proteins with specific components of the skeleton have measurable impact on the rheologic properties of the RBC. The nature of the cellular perturbation depends on the particular characteristics of the parasite protein itself and the RBC protein with which it interacts. For example, direct binding of KAHRP to the repeat 4 domain of α-spectrin[29] and the formation of membrane knobs,[6] or the interaction of PfEMP3 with spectrin and actin,[30] causes a dramatic increase in the rigidity of iRBCs,[7] presumably by limiting the normal intrinsic molecular flexibility of the spectrin polymer.

Interestingly, with the exception of the major cytoadherence ligand PfEMP1, none of the other exported proteins that interact with the RBC membrane skeleton appear to be exposed on the surface of the iRBC; yet, in addition to alteration of the mechanical properties of iRBCs, they also can have profound effects on iRBC adhesion, which must occur either by some secondary, indirect mechanism or altered trafficking of PfEMP1 to the RBC surface. In the case of KAHRP, defective anchoring of PfEMP1 in the iRBC membrane seems the most likely mechanism because we have previously demonstrated high-affinity interactions between specific domains of KAHRP and the cytoplasmic tail of PfEMP1,[31] and iRBCs not expressing KAHRP show dramatically reduced adhesion under flow, but not under static conditions.[6]

Although Pf332 was first described by Mattei and Scherf[9] more than a decade ago as a giant, megadalton protein exported from malaria parasites into RBCs, its function has remained enigmatic. Studies of this protein have remained scanty largely as the result of its extreme size, high net negative charge, and presence of extensive blocks of repeated sequences. Our generation of a set of transgenic parasite clones in which Pf332 expression had been truncated or ablated has allowed the first functional analysis of Pf332 in iRBCs. Although Pf332 has been detected in all clinical parasite isolates surveyed to date,[9,32] complete ablation of its expression in transgenic parasites reveals that it is not essential for parasite replication in vitro, nor does it appear to be involved in the process of RBC invasion because our transgenic KO parasite clones show normal multiplication rates (data not shown). Instead, our data suggest that Pf332 is involved in altered rheologic properties of iRBCs and may thus be essential in vivo to protect iRBCs from clearance by the spleen. The absence of Pf332 leads to several changes in iRBCs. MCs show striking morphologic alterations, adopting a stacked and aggregated appearance in RBCs infected with mature parasites. iRBCs lacking Pf332 adhere to CD36 at a significantly lower level and, this behavior is consistent with a reduced amount of PfEMP1 present on the iRBC surface. Finally, the protein has a remarkable effect on the altered mechanical properties of iRBCs by specifically modulating the rigidity of the RBC membrane skeleton.

Because we have generated both KO and truncated forms of Pf332, we are able to assign different functional roles to different regions of the protein. Maintenance of normal MC morphology, as

well as in iRBC adhesion and trafficking of PfEMP1 from MCs to the iRBC surface, requires the regions of Pf332 upstream of residue 2965. The sequences involved in moderating rigidity of the RBC membrane, however, lie in regions between residue 3246 and the C terminus of the protein. Reduced iRBC adhesion observed in Pf332 KO parasites could be the result of the loss of an externally exposed DBL-binding domain, as has been suggested recently by others.[10] Our data do not support this but rather suggest that the DBL domain is not externally exposed on the RBC. We base this on localization studies using antibodies raised against the extreme N terminus of Pf332 (containing the DBL domain) in either intact or permeabilized iRBC, which place the protein at the MCs, within the RBC cytoplasm, and not at the RBC surface. We have also attempted to directly observe Pf332 on the RBC surface both by live IFA using the N-terminal directed antibody and by immunoblotting for a protease-sensitive fragment of Pf332, which would be cleaved after treatment of intact iRBCs with trypsin. In neither experiment could we detect any externally exposed Pf332, leading us to conclude that there is very little or none exposed on the RBC surface (data not shown).

We postulate that the DBL domain of Pf332 is likely to be found in the interior of the MC and is acting as some form of protein association domain, perhaps with specific domains of PfEMP1. Thus, the defect in adhesion in Pf332-null parasites may be caused by diminished trafficking of PfEMP1 to the surface because it is incorrectly stabilized within the lumen of the MCs. Alternatively, the abnormal morphology and location of the MC may make it more difficult for PfEMP1 to exit correctly and translocate onto the RBC surface. This was the likely mechanism of loss of adhesion by SBP1-null parasites in which the absence of SBP1 prevented docking of MCs to the RBC membrane skeleton with consequent effects on PfEMP1 translocation onto the RBC surface.[27]

Finally, we also do not believe that the reduced ability of Pf332 KO iRBCs to adhere could be the result of a possible *var* gene switching event during the parasite derivation or cloning process and consequent expression of a different surface PfEMP1 with altered affinity for CD36. First, almost all *var* genes encode PfEMP1 that bind to CD36 (the adhesion assay we performed) so that switching would be unlikely to affect the measurement. Most compelling, however, is the observation that all 4 independent KO clones showed reduced adhesion and all 4 independent truncation mutants adhered at wild-type levels, suggesting that only complete loss of the gene would lead to decreased adherence ($P < .03$ by Fisher exact test).

The role of Pf332 in the maintenance of normal MC morphology is intriguing. It is possible that the large (5533 residue), highly negatively charged (pI = 3.79) cytoplasmic domain of Pf332 may play a role in separating MCs as they are formed and therefore, in the absence of Pf332, MCs aggregate into multilamellar stacks. Consistent with this hypothesis is our observation that in the truncation mutants that have a reduced yet still highly charged cytoplasmic domain (pI ~3.70) almost identical to that for the full-length protein (3.79), MCs do not aggregate and exhibit normal, wild-type single lamellae morphology. However, very little is known about the process of MC budding, formation, or maturation, and more information is required before a detailed mechanism can be suggested.

In contrast to other exported parasite proteins, whose role in the alteration of the mechanical properties of the infected RBC is to increase membrane rigidity, Pf332 is the first protein to be described whose function appears to be to moderate the level of membrane skeleton rigidity induced by the parasite. The precise

mechanism for this presently remains unclear. It may arise as a result of interference with a direct interaction between Pf332 and the RBC membrane skeleton or indirectly. A substantial proportion of MCs are tethered directly to the membrane skeleton,[22] and this would bring the 5533 residue, highly negatively charged cytoplamic tail of Pf332 in close proximity to proteins of the membrane skeleton.

In fact, our results here (Figure 2A) demonstrate that a substantial proportion of Pf332 is found in the Triton X-100 insoluble fraction in detergent-solubilized iRBCs. This supports a direct association between this protein and the RBC membrane skeleton. Finally, we have recent unpublished observations that a specific domain of Pf332 binds directly to actin in the RBC membrane skeleton providing a plausible mechanism as to how Pf332 can modify the membrane mechanical properties of the RBC. This would be in accord with the general means by which other exported malaria proteins affect the RBC membrane skeleton (see Cooke et al[1] for review). It remains possible that the absence of the C-terminal half of Pf332, which is an extremely large protein, may expose more binding sites on the membrane skeleton for other exported proteins including PfEMP3 and KAHRP. As both of these proteins are involved in RBC rigidification,[7,29,33] the net effect of this would be an overall increase in RBC rigidity, exactly as was observed. We have attempted to examine this possibility by silver staining of Triton X-100–insoluble/SDS soluble fractions of iRBCs, but we cannot detect any obvious increases in these protein profiles, at least by this perhaps relatively insensitive method (Figure S3).

At present, we favor the mechanism that suggests membrane properties are altered as a result of direct binding, but further work is required to confirm this hypothesis. Functional characterization of exported malaria proteins continues to reveal a complex interplay of protein interactions at the membrane skeleton. Most of these proteins appear to be playing important roles in the pathogenesis of falciparum malaria by structural and functional alterations to RBCs. Methods of interfering with these alterations may provide novel methods of lessening pathology associated with infection.

Authorship

Contribution: F.K.G. and K.M.F. performed the experiments; E.H. performed the electron microscopy; F.K.G., K.M.F., L.M.K., and B.M.C. analyzed results and made figures; B.M.C., R.L.C., and N.M. designed and directed the research; and F.K.G., L.M.K., R.L.C., and B.M.C. wrote the paper.

Conflict-of-interest disclosure: The authors declare no competing financial interests.

Correspondence: Brian M. Cooke, Department of Microbiology, Monash University, Victoria 3800, Australia; e-mail: brian.cooke@med.monash.edu.au.

References

1. Cooke BM, Mohandas N, Coppel RL. Malaria and the red blood cell membrane. Semin Hematol. 2004;41:173-188.

2. Kraemer SM, Smith JD. A family affair: *var* genes, PfEMP1 binding, and malaria disease. Curr Opin Microbiol. 2006;9:374-380.

3. Hiller NL, Bhattacharjee S, van Ooij C, et al. A host-targeting signal in virulence proteins reveals a secretome in malarial infection. Science. 2004; 306:1934-1937.

4. Marti M, Good RT, Rug M, Knuepfer E, Cowman AF. Targeting malaria virulence and remodeling proteins to the host erythrocyte. Science. 2004; 306:1930-1933.

5. Bhattacharjee S, van Ooij C, Balu B, Adams JH, Haldar K. Maurer's clefts of Plasmodium falciparum are secretory organelles that concentrate virulence protein reporters for delivery to the host erythrocyte. Blood. 2008;111:2418-2426.

6. Crabb BS, Cooke BM, Reeder JC, et al. Targeted gene disruption shows that knobs enable malaria-infected red cells to cytoadhere under physiological shear stress. Cell. 1997;89:287-296.

7. Glenister FK, Coppel RL, Cowman AF, Mohandas N, Cooke BM. Contribution of parasite proteins to altered mechanical properties of malaria-infected red blood cells. Blood. 2002;99:1060-1063.

8. Waller KL, Nunomura W, An X, Cooke BM, Mohandas N, Coppel RL. Mature parasite-infected erythrocyte surface antigen (MESA) of Plasmodium falciparum binds to the 30-kDa domain of protein 4.1 in malaria-infected red blood cells. Blood. 2003;102:1911-1914.

9. Mattei D, Scherf A. The Pf332 gene of Plasmodium falciparum codes for a giant protein that is translocated from the parasite to the membrane of infected erythrocytes. Gene. 1992;110:71-79.

10. Moll K, Chêne A, Ribacke U, et al. A novel DBL-domain of the P falciparum 332 molecule possibly involved in erythrocyte adhesion. PLoS ONE. 2007;2:e477.

11. Hinterberg K, Scherf A, Gysin J, et al. Plasmodium falciparum: the Pf332 antigen is secreted from the parasite by a brefeldin A-dependent pathway and is translocated to the erythrocyte membrane via the Maurer's clefts. Exp Parasitol. 1994;79:279-291.

12. Udomsangpetch R, Carlsson J, Wahlin B, et al. Reactivity of the human monoclonal antibody 33G2 with repeated sequences of three distinct Plasmodium falciparum antigens. J Immunol. 1989;142:3620-3626.

13. Ahlborg N, Iqbal J, Bjork L, Stahl S, Perlmann P, Berzins K. Plasmodium falciparum: differential parasite growth inhibition mediated by antibodies to the antigens Pf332 and Pf155/RESA. Exp Parasitol. 1996;82:155-163.

14. Cranmer SL, Magowan C, Liang J, Coppel RL, Cooke BM. An alternative to serum for cultivation of Plasmodium falciparum in vitro. Trans R Soc Trop Med Hyg. 1997;91:363-365.

15. Waterkeyn JG, Cowman AF, Cooke BM. Plasmodium falciparum: gelatin enrichment selects for parasites with full-length chromosome 2. Implications for cytoadhesion assays. Exp Parasitol. 2001;97:115-118.

16. Duraisingh MT, Triglia T, Cowman AF. Negative selection of Plasmodium falciparum reveals targeted gene deletion by double crossover recombination. Int J Parasitol. 2002;32:81-89.

17. Crabb BS, Triglia T, Waterkeyn JG, Cowman AF. Stable transgene expression in Plasmodium falciparum. Mol Biochem Parasitol. 1997;90:131-144.

18. Fidock DA, Wellems TE. Transformation with human dihydrofolate reductase renders malaria parasites insensitive to WR99210 but does not affect the intrinsic activity of proguanil. Proc Natl Acad Sci U S A. 1997;94:10931-10936.

19. Wu Y, Kirkman LA, Wellems TE. Transformation of Plasmodium falciparum malaria parasites by homologous integration of plasmids that confer resistance to pyrimethamine. Proc Natl Acad Sci U S A. 1996;93:1130-1134.

20. Anderluh G, Pungercar J, Strukelj B, Macek P, Gubensek F. Cloning, sequencing, and expression of equinatoxin II. Biochem Biophys Res Commun. 1996;220:437-442.

21. Jackson KE, Spielmann T, Hanssen E, et al. Selective permeabilization of the host cell membrane of Plasmodium falciparum-infected red blood cells with streptolysin O and equinatoxin II. Biochem J. 2007;403:167-175.

22. Hanssen E, Hawthorne P, Dixon MW, et al. Targeted mutagenesis of the ring-exported protein-1 of Plasmodium falciparum disrupts the architecture of Maurer's cleft organelles. Mol Microbiol. 2008;69:938-953.

23. Beeson JG, Chai W, Rogerson SJ, Lawson AM, Brown GV. Inhibition of binding of malaria-infected erythrocytes by a tetradecasaccharide fraction from chondroitin sulfate A. Infect Immun. 1998;66:3397-3402.

24. Cooke BM, Glenister FK, Mohandas N, Coppel RL. Assignment of functional roles to parasite proteins in malaria-infected red blood cells by competitive flow-based adhesion assay. Br J Haematol. 2002;117:203-211.

25. Cooke BM, Coppel RL, Nash GB. Analysis of the adhesive properties of Plasmodium falciparum-infected red blood cells under conditions of flow. Methods Mol Med. 2002;72:561-569.

26. Cooke BM, Coppel RL, Nash GB. Preparation of adhesive targets for flow-based cytoadhesion assays. Methods Mol Med. 2002;72:571-579.

27. Cooke BM, Buckingham DW, Glenister FK, et al. A Maurer's cleft-associated protein is essential for expression of the major malaria virulence antigen on the surface of infected red blood cells. J Cell Biol. 2006;172:899-908.

28. Sargeant TJ, Marti M, Caler E, et al. Lineage-specific expansion of proteins exported to erythro-cytes in malaria parasites. Genome Biol. 2006;7: R12.

29. Pei X, An X, Guo X, Tarnawski M, Coppel R, Mohandas N. Structural and functional studies of interaction between Plasmodium falciparum knob-associated histidine-rich protein (KAHRP) and erythrocyte spectrin. J Biol Chem. 2005;280: 31166-31171.

30. Waller KL, Stubberfield LM, Dubljevic V, et al. Interactions of Plasmodium falciparum erythrocyte membrane protein 3 with the red blood cell membrane skeleton. Biochim Biophys Acta. 2007; 1768:2145-2156.

31. Waller KL, Cooke BM, Nunomura W, Mohandas N, Coppel RL. Mapping the binding domains involved in the interaction between the Plasmodium falciparum knob-associated histidine-rich protein (KAHRP) and the cytoadherence ligand P falciparum erythrocyte membrane protein 1 (PfEMP1). J Biol Chem. 1999;274:23808-23813.

32. Haddad D, Snounou G, Mattei D, et al. Limited genetic diversity of Plasmodium falciparum in field isolates from Honduras. Am J Trop Med Hyg. 1999;60:30-34.

33. Pei X, Guo X, Coppel R, Mohandas N, An X. Plasmodium falciparum erythrocyte membrane protein 3 (PfEMP3) destabilizes erythrocyte membrane skeleton. J Biol Chem. 2007;282: 26754-26758.